Full Length Article

Above knee socket prosthesis use changes proximal femur morphology

Galen F. Roda [a], Jason W. Stoneback [b], David Gimarc [c], Brecca M.M. Gaffney [a,d,*]

[a] Department of Mechanical Engineering, University of Colorado Denver, Denver, CO, United States of America
[b] Department of Orthopedics, University of Colorado School of Medicine, Aurora, CO, United States of America
[c] Department of Radiology, University of Colorado School of Medicine, Aurora, CO, United States of America
[d] Center for Bioengineering, University of Colorado Anschutz Medical Campus, Aurora, CO, United States of America

ARTICLE INFO

ABSTRACT

Patients with transfemoral amputation (TFA) are up to six times more likely to develop hip osteoarthritis (OA) in either or both the intact and residual limb, which is primarily attributed to habitually altered joint loading due to compensatory movement patterns. However, joint loading patterns differ between limbs, which confounds the understanding of loading-induced OA etiology across limbs. It remains unknown if altered loading due to amputation results in bony shape changes at the hip, which is a known etiological factor in the development of hip OA. Retrospective computed tomography images were collected of the residual limb for 31 patients with unilateral TFA (13F/18M; age: 51.7 ± 9.9 y/o; time since amputation: 13.7 ± 12.4 years) and proximal femur for a control group of 29 patients (13F/16M; age: 42.0 ± 12.27 years) and used to create 3D geometries of the proximal femur. Femoral 3D geometric variation was quantified using statistical shape modeling (SSM), a computational tool which placed 2048 corresponding particles on each geometry. Independent modes of variation were created using principal component analysis. 2D radiographic measures of the proximal femur, including common measures such as α-angle, head neck offset, and neck shaft angle, were quantified on digitally reconstructed radiographs (DRRs). SSM results were then compared to 2D measures using Pearson correlation coefficients (r). Two-sample t-tests were used to determine if there were significant differences between the TFA and control group means of 2D radiographic measurements ($p < 0.05$). Patients with TFA had greater femoral head asphericity within the SSM, which was moderately correlated to head-neck offset ($r = -0.54$) and α-angle ($r = 0.63$), as well as greater trochanteric torsion, which was strongly correlated to the novel radiographic measure of trochanteric torsion ($r = -0.78$), compared to controls. For 2D measures, the neck-shaft angle was smaller in the TFA group compared to the control group ($p = 0.01$) while greater trochanter height was larger in the TFA group compared to the control group ($p = 0.04$). These results indicate altered loading from transfemoral prosthesis use changes proximal femur bony morphology, including femoral head asphericity and greater trochanter changes. Greater trochanter morphologic changes, though not a known factor to OA, affect moment arm and line of action of the primary hip abductors, the major muscles which contribute to joint loading and hip stability. Thus, chronic altered loading of the amputated limb hip, whether under- or overloading, results in bony changes to the proximal femur which may contribute to the etiological progression and development of OA.

1. Introduction

The number of Americans living with limb loss is expected to nearly double from approximately 2.2 million to 3.6 million by the year 2050 due to an aging population and growing prevalence of dysvascular conditions [1]. Within this population, persons with transfemoral amputation (TFA) have lower levels of physical function and mobility compared to persons with transtibial amputation [2,3]. One contributing factor to lower physical function is the increased risk of secondary conditions, including low back pain, osteopenia, osteoporosis, and osteoarthritis (OA) [4]. Hip OA is especially prevalent in persons with TFA, compared to able-bodied individuals, as they are three- to six- fold

more likely to develop hip OA [4–7]. OA causes persistent pain that severely impedes mobility, daily activity, and overall quality of life leading to a 20 % higher age-adjusted mortality rate [8,9].

The three primary etiological factors of OA involve mechanical, biologic, and metabolic pathways that all contribute to cartilage degeneration [10]. Specifically, it is widely agreed that habitually increased joint loading is a primary contributor to OA development in the intact limb in persons with TFA [5,11–13]; however, prior studies disagree if joint loading decreases [11,14,15] or increases [16] in the amputated limb. Nonetheless, amputated limb hip OA has been estimated to occur in upwards of 55 % of older patients with TFA [7]. Therefore, it is likely that there are other mechanical factors, including those induced from altered joint loading, that contribute to the etiology of OA but have not been as rigorously explored within this population.

Chronic change in the mechanical stimulus applied to bone through altered loading can result in both bone mineral density and morphological changes [17], as seen after long-term space flight, prolonged bedrest, and in idiopathic torsional deformities [18–20]. Although prior evidence has established that the amputated limb has lower bone mineral density in patients with TFA [21], less is known about its morphology in this population. Changes in bony morphology are an important etiological factor in hip OA as they alters intra-articular mechanics [22]. It is well-documented that external loads (e.g., ground reaction forces) are different in the TFA population [11–16], yet the loading applied to the proximal femur is also dependent upon internal (e.g., muscle) forces. Specifically, muscle forces are one of the main contributors to hip joint loading [23] and the resulting strain in the femur [20,24]. Thus, any changes in muscle forces could potentially contribute to bony remodeling, and thus changes in morphology. Unfortunately, patients with TFA demonstrate substantial amputated limb hip muscle weakness, which is commonly attributed to limb disuse within the socket [25]. However, despite changes to both internal and external factors in patients with TFA which contribute to loading, it remains unknown how these changes in loading result in morphological changes of the proximal femur.

Quantifying three-dimensional (3D) bony morphology is critical to improve the understanding of the etiological contribution of morphological changes to joint damage. Recent progress has been made toward the use of quantifying 3D shape using reconstructions generated from volumetric images (e.g., computed tomography (CT)), yet objective quantification of 3D morphologic variation remains difficult. Statistical shape modeling (SSM) has emerged as a powerful tool to objectively quantify complex morphology [26]. SSM has previously been utilized to quantify 3D bony geometric variation that contributes to OA pathomechanics in pre-arthritic OA populations, including patients with femoroacetabular impingement [27,28], hip dysplasia [29], Legg-Calvé-Perthes disease [30], and slipped capital femoral epiphysis [30], yet has not been used to determine if bony morphological abnormalities are prevalent in patients with TFA.

Despite advancements in imaging technology, hip OA is commonly diagnosed based on discrete two-dimensional (2D) radiographic measures due to the convenience and cost-effectiveness of radiographs [31]. Joint space narrowing and presence of osteophytes are radiographic indicators of OA and occur after irreparable articular damage has occurred [9,32]. Therefore, 2D radiographic measures are not sensitive to early detection of osteoarthritic changes, when interventional therapies may be most effective in symptom mitigation and prevention of further cartilage degeneration [9]. Three-dimensional bony shape changes have previously been shown to precede the later onset of 2D radiographic evidence of OA [33]. Thus, robust 3D quantification of the proximal femur bony morphology is necessary to identify OA risk.

Therefore, the primary objective of this investigation was to determine if residual proximal femur morphology was different between patients with TFA and an able-bodied control group using SSM and volumetric image data. Our secondary objective was to then relate 3D shape variability to common 2D radiographic measurements relevant to hip OA for both groups to increase clinical interpretation of our findings. We hypothesized that both the mean shape and the modes of shape variation would differ between groups, indicating that the chronically altered loading caused by long-term prosthesis use causes changes in bony hip morphology.

2. Materials and methods

2.1. Data acquisition, 3D surface reconstruction, preprocessing

With Institutional Review Board approval, volumetric CT images of the residual limb were retrospectively identified from 31 patients with unilateral TFA (13F/18M; age: 51.7 ± 9.9 y/o; time since amputation: 13.7 ± 12.4 years). Patients with bilateral amputation or previous pelvic/hip surgery, fracture, or infection were excluded. A control group was created by retrospectively identifying CT images of 29 able-bodied patients who visited the emergency room in our institution (13F/16M; age: 42.0 ± 12.27 years). Inclusion criteria for control images included: CT scan including proximal femur, no total hip arthroplasty, and no lower-limb amputation.

The proximal femur (residual for TFA and right for control) was segmented from the volumetric CT image data using a previously validated method with semi-automatic thresholding (Amira v5.4, Thermo Scientific, Waltham, MA) (Fig. 1) [29]. Three-dimensional proximal femur reconstructions were triangulated from the segmentation and slightly smoothed with built-in Amira tools to remove segmentation artifacts. All geometries were aligned to a neutrally aligned master femur using an iterative closest point algorithm and rigidly scaled to minimize root mean square distance between proximal femur surfaces. The 3D surface reconstructions were then cropped at the superior aspect of the lesser trochanter in order to minimize shape variation caused by femoral shaft length [28]. Cropped proximal femurs were then realigned and rigidly scaled to the cropped neutral master femur.

2.2. Statistical shape models

Statistical shape models (SSMs) were created by placing particles of corresponding positions across each geometry for both the TFA and control group (Fig. 1). Specifically, 2048 particles were placed on each proximal femur surface with a correspondence method that automatically performs particle initialization and then utilizes hierarchical splitting and variational formulation of ensemble entropy to optimize correspondence particle position (ShapeWorks) (Fig. 1) [34]. Placement of correspondence particles was optimized on each surface using a gradient descent energy function to create a compact and accurate distribution of samples in shape space, as previously done in other populations [28–30,35–37]. Three SSMs were created: 1) a combined SSM, 2) one for the TFA group, and 3) one for the control group. The combined SSM was used to determine if the mean shape was different per group and independent SSMs were used to determine if the prevalence of specific type of morphological variability differed between groups, as previously used [28,29].

2.3. Digitally reconstructed radiographs

Digitally reconstructed radiographs (DRR) of the proximal femur were created using a ray-casting technique from CT image data to emulate a 2D radiograph, as previously described [38–40]. Three separate DRR views were created, two commonly used in clinical radiographic settings (anteroposterior and frog-leg lateral view) and a top-down axial projection. Specifically, the three DRR views created were: 1) a standing anteroposterior (AP) view, with 15° internal hip rotation, 2) a simulated superoinferior view, and 3) a frog-leg lateral view (35° hip flexion and 60° hip external rotation) [41]. From each view, 2D radiographic measurements were made by a board-certified musculoskeletal radiologist (DG) (Fig. 2). Measurements made on the
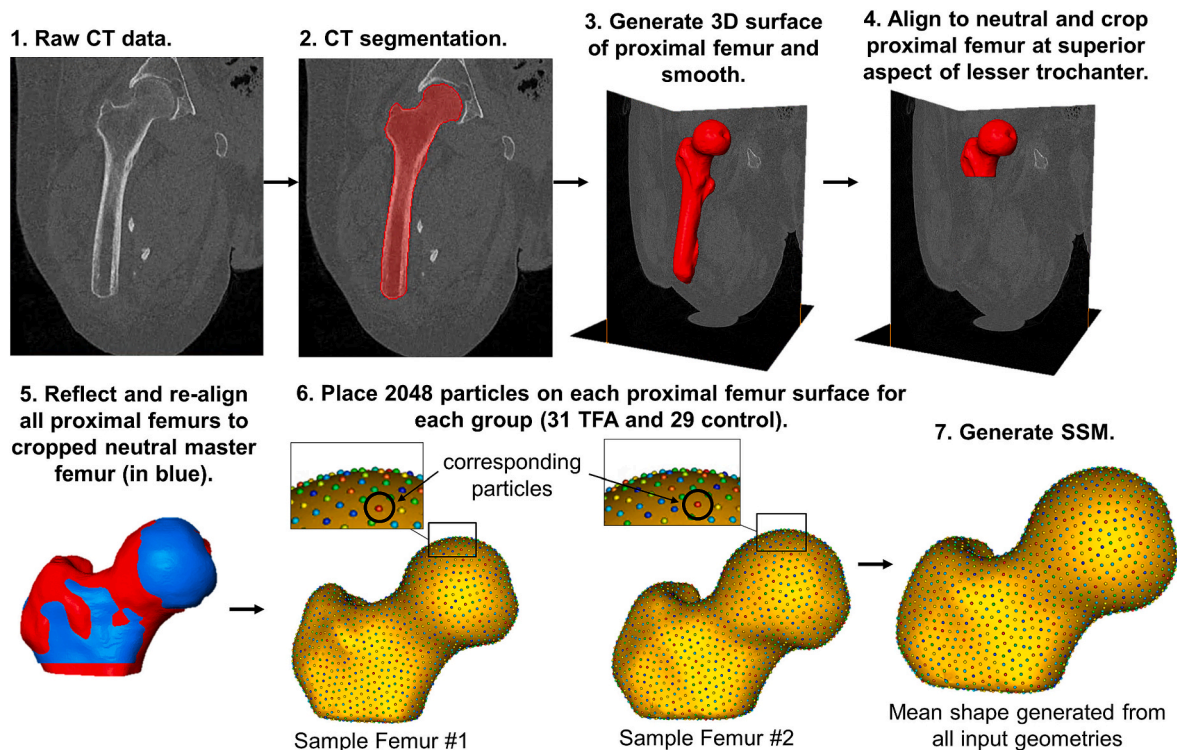
Fig. 1. Statistical shape modeling (SSM) workflow. CTs were used to create 3D proximal femur reconstructions and 2048 correspondence particles are placed on each surface.

AP view included femoral neck length, greater trochanter width, neck-shaft angle, and greater trochanter height (Fig. 2a). On the axial view, greater trochanter offset, greater trochanter angle, lesser trochanter angle, and greater trochanter-lesser trochanter angle were measured (Fig. 2b). Head-neck offset and α-angle were measured using the frog-leg lateral view (Fig. 2c). Further descriptions of each measure are detailed within the Supplemental Material.

2.4. Statistical analysis

Principal component analysis (PCA) was used to reduce the dimensionality of the SSM by identifying primary, independent modes of variation [42]. PCA determines uncorrelated modes of variation by determining orthonormal eigenvectors and then ranks them according to the amount of variance explained based on the magnitude of the eigenvalue, which is considered an independent "mode" of variation, detailed mathematically in [43,44]. PCA was performed on each SSM to create distinct primary, independent modes of variation between groups. Parallel analysis was then used to quantify the statistically significant number of shape modes for each SSM. In parallel analysis, PCA modes are considered nonspurious if their eigenvalues are greater than those of a respective random data set with the same number of variables and samples [45].

A Hotelling T^2 test with false discovery rate reduction was used to compare the mean shape between groups with a null hypothesis that corresponding particles would be sampled from the same distribution using the combined SSM. PCA loading values, a scale factor which describes how the individual shape varies from the mean shape within a specific shape mode [46], from the combined SSM were compared across groups using two-sample *t*-tests.

Two-dimensional radiographic measurements were compared across groups using two-sample *t*-tests. Additionally, the relation between SSM modes of variation and radiographic measures was determined by correlating the PCA loading value from the distinct group SSMs to each radiographic measure using Pearson's correlation coefficient (*r*).

Absolute value of correlation coefficients were categorized as uncorrelated ($r < 0.25$), fairly correlated ($0.25 \leq |r| < 0.50$), moderately correlated ($0.5 \leq |r| < 0.75$), or highly correlated ($0.75 \leq |r| \leq 1.0$) and 95 % confidence intervals were calculated [47]. Confidence intervals that did not cross zero were considered statistically significant [48]. The level of significance was set at 0.05 for all inferential statistics.

3. Results

3.1. Statistical shape model

Significant morphological differences were found between the control and TFA mean shapes (Fig. 3). Differences occurred along the inferomedial portion of the femoral neck as well as the superomedial and anteromedial region of the femoral head, indicating greater femoral head asphericity within the TFA group (Fig. 3).

Parallel analysis determined the first five modes (82.2 % total variance) were significant (i.e., non-spurious) for the TFA group while the first four modes (77.9 % total variance) were significant for the control group (Fig. 4).

No significant differences were found between the PCA loading values between groups from the combined SSM. However, when assessed independently, differences emerged between groups that indicate difference in prominence of shape variability type (i.e., order of mode) between groups. Mode 1 accounted for 32.69 % and 38.02 % of the variance for TFA and control group, respectively. For both groups, despite cropping and rigid scaling, mode 1 described size variability, most noticeably in the AP view (Fig. 5). Additionally, mode 1 described change in greater trochanteric shape and asphericity of the femoral head, yet the magnitude of variation was more pronounced in the TFA group (Fig. 5). Mode 2 accounted for 25.57 % and 22.33 % of the variance for TFA and control group, respectively. In mode 2, the TFA group had increased head-neck offset variation and increased variation of the greater trochanter width while the control group had increased variation in greater trochanteric height (Fig. 5). Mode 3 accounted for
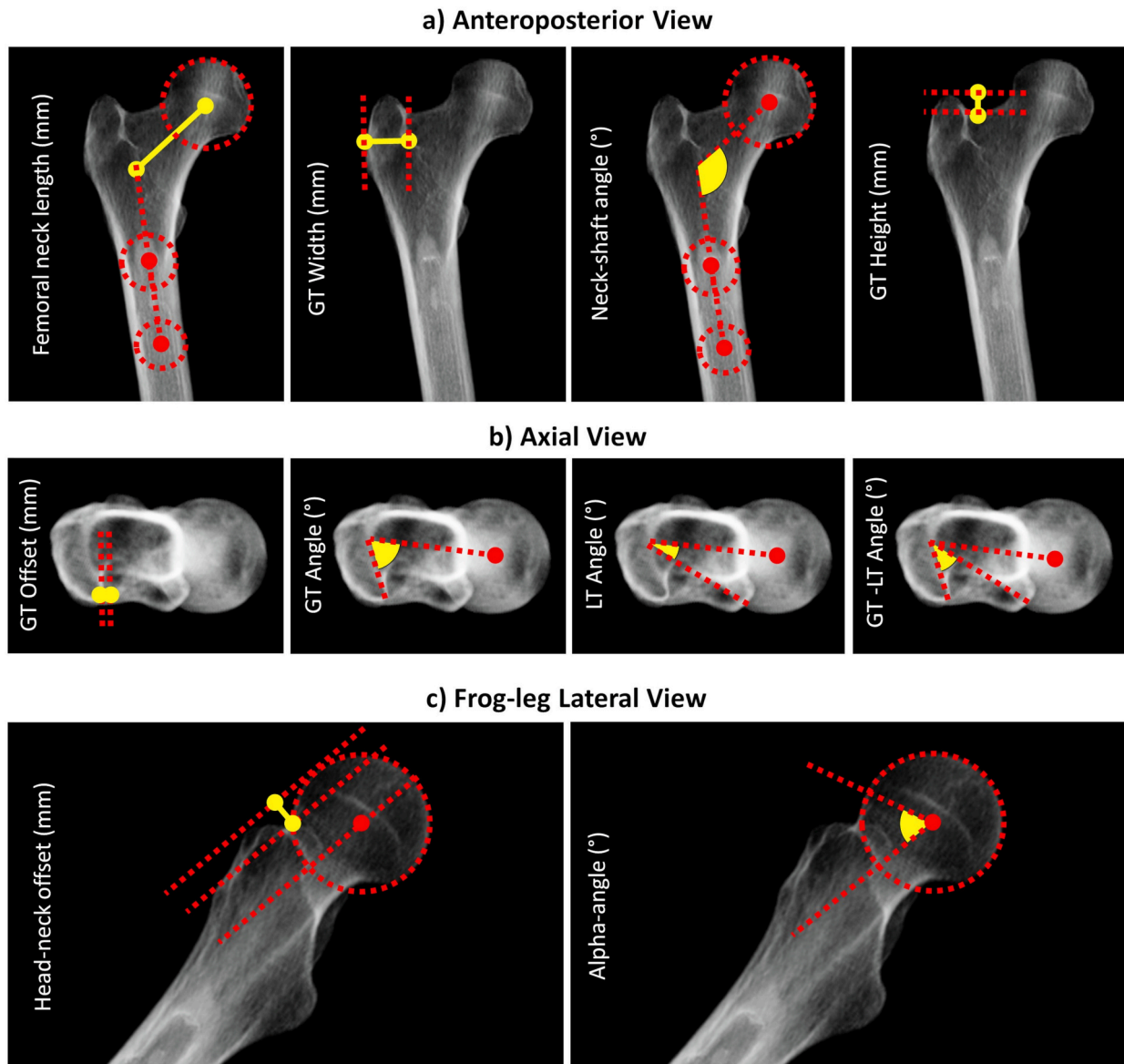
Fig. 2. Digitally reconstructed radiographic views and measurements. Three radiographic views, a) anteroposterior, b) axial, and c) frog-leg lateral, were digitally reconstructed from CT and the 2D measures were made on corresponding views.
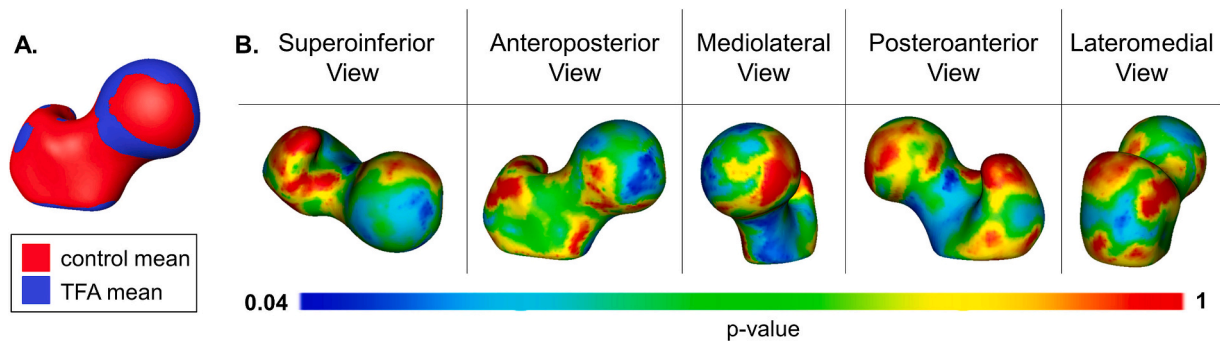
Fig. 3. Mean shape differences. A) Mean proximal femur shape from the SSM for the TFA group (blue) imposed on the control group mean shape (red). B) The color map is given on the mean proximal femur shape of the control group and displays group-wise *p*-values for differences between the mean TFA and control shapes, with areas in blue indicating statistically different shapes (*p* < 0.05). (For interpretation of the references to color in this figure legend, the reader is referred to the web version of this article.)
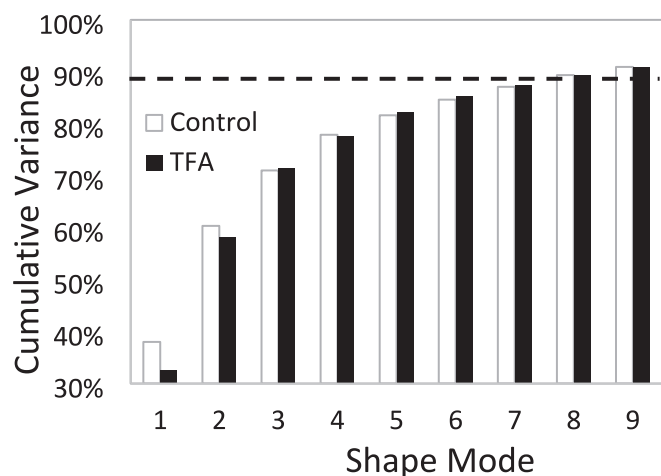
Fig. 4. Resultant cumulative variance for all SSMs. The first nine modes account for 90.9 % of the variance within the control group, 91.0 % of the variance within the TFA group. The dotted line indicates 90 % VAF, commonly reported for SSMs [28,30].

13.16 % and 10.67 % of the variance for TFA and control respectively. For both groups, mode 3 described femoral neck shape (Fig. 5). Mode 4 accounted for 6.12 % and 6.87 % for TFA and control respectively. In the TFA group, mode 4 described greater trochanteric torsion while in the control group, mode 4 described greater trochanter height (i.e., greater trochanteric superior offset) (Fig. 5). Mode 5 accounted for 4.69 % of the variance within the TFA group, which described variation in the greater trochanter as well as concavity of the femoral neck at the head-neck junction, and was not statistically significant for the control group (Fig. 5). Three-dimensional videos displaying shape variability for all non-spurious modes for both groups are included in the Supplemental Material.

3.2. Radiographic measurements from DRR

The neck-shaft angle was smaller in the TFA group ($129.2 \pm 5.2°$) compared to the control group ($132.7 \pm 4.0°$) ($p = 0.006$). The greater trochanter height was larger in the TFA group (7.8 ± 1.9 mm) compared to the control group (6.7 ± 2.1 mm) ($p = 0.044$). No other differences were found between groups in 2D measurements (Table 1).

3.3. SSM and DRR correlation

For control group, mode 1 was fairly correlated to the novel greater trochanter-lesser trochanter (GT-LT) angle ($r = -0.42$, $p = 0.02$) (Table 2). For the TFA group, mode 2 was moderately correlated to both head-neck offset ($r = -0.54$, $p < 0.01$) and α-angle ($r = 0.63$, $p < 0.01$) (Table 2). For the control group, mode 2 was fairly correlated to greater trochanter height ($r = -0.42$, $p = 0.02$). For both groups, mode 3 was fairly correlated to femoral neck length for the TFA and control group ($r = 0.40$, $p = 0.02$ and $r = 0.49$, $p < 0.01$ respectively). For the control group, mode 3 was also moderately correlated to 2D measurements of greater trochanter width ($r = 0.66$, $p < 0.01$), and fairly correlated to both greater trochanter medial offset ($r = 0.48$, $p < 0.01$) and greater trochanter angle ($r = -0.42$, $p = 0.02$). For the TFA group, mode 4 was highly correlated with a 2D measurement describing the greater trochanter torsion relative to the femoral neck axis in the TFA group ($r = -0.78$, $p < 0.01$) (Fig. 4) while, for the control group, mode 4 was moderately correlated to greater trochanter height ($r = -0.62$, $p < 0.01$) and fairly correlated to GT-LT angle ($r = -0.40$, $p = 0.03$). Finally, mode 5 was fairly correlated to the 2D measurement for head neck shaft angle in the TFA group ($r = -0.46$, $p < 0.01$).

4. Discussion

The objective of this investigation was to determine how amputated limb proximal femur morphology in patients with TFA differed from able-bodied controls. Our results indicated that the amputated limb proximal femur in patients with TFA had greater variability in the shape of the femoral head and greater trochanter compared to controls. Moreover, when compared to an able-bodied control group, the mean morphology of the femurs was different. We attribute the differences in morphological variability in the TFA group to well-documented habitual asymmetric limb-loading patterns [12,14–16,25,49–51]. Furthermore, as radiographs remain a common tool used in clinical orthopedic settings due to the ease and cost (healthcare and computational) [43], our second objective was to relate SSM results to common radiographic measurements to objectively translate findings into clinical context [44]. We found significant correlations between 3D shape variability and 2D radiographic measures associated with femoral head asphericity and greater trochanteric shape in the TFA group. These results highlight the importance of quantifying 3D shape variation to better the understanding of limb-dependent OA etiology in this at-risk population.

Our results indicated that patients with TFA have greater variability in femoral head shape in the amputated limb compared to controls. Clinically, it is well established that changes in femoral head asphericity are an etiological factor for OA development as it can pathologically alter intra-articular mechanics [52], commonly observed in patients with femoroacetabular impingement [53]. Although there is no clear underlying mechanistic understanding as to why femoral head asphericity occurs in the able-bodied population, we primarily attribute femoral head asphericity in the TFA group to chronically altered loading applied to the hip joint. As the force transmission is altered between the ground and residual limb within a traditional socket-suspended prosthesis [12,14–16,49–51], the load applied to residual femur is altered [54], and thus the load to the hip joint is altered [55]. This altered load transmission to the hip can be exacerbated by malalignment of the residual femur within the socket, most commonly abduction and external rotation of the residual femur, commonly observed in patients with TFA. This is caused by antagonistic muscle imbalance as the adductor musculature are altered during surgery while the abductors are preserved [56]. Over time, this malalignment will result in lower physiological function of the abductors, loss of muscle force, and reduction in frontal plane hip joint moment, all of which will alter hip joint loading [57]. Furthermore, compensatory movement patterns commonly adopted by patients with TFA to aid in stability and propulsion in the absence of the ankle and knee joints, such as compensated Trendelenburg and increased hip flexion [58–60], also contribute to altered loading within the hip joint. Collectively, these factors that all contribute to altered hip joint loading alter the mechanical stimulus on the femoral head, which causes adaptation in the bone microstructure and eventually macrostructure (i.e., shape).

Patients with TFA also demonstrated greater variability in greater trochanteric torsion compared to controls. This is of clinical relevance as it directly impacts paths of the primary hip abductors (e.g., gluteus medius, gluteus minimus) as the greater trochanter is the insertion site for these muscles. Because these muscles are primary contributors to hip joint loading [23], these results may suggest that geometric changes to the muscle path in addition to strength changes play a role in altered joint loading in this population. For example, it has previously been shown that changes to abductor muscle line of action and moment arm impacts hip joint loading [50]. Although the abductors are not directly affected by transfemoral amputation, prior evidence has shown that abductor muscle weakness is greater in the amputated limb in patients with TFA compared to the intact limb or controls [49,58]. Furthermore, abductor weakness has also been linked to the development of OA [61], as hip abductor weakness causes increased hip joint loading [62]. Therefore, because the abductors are critical for limb stability within the socket [58,63] and healthy joint loading [23], abductor strengthening
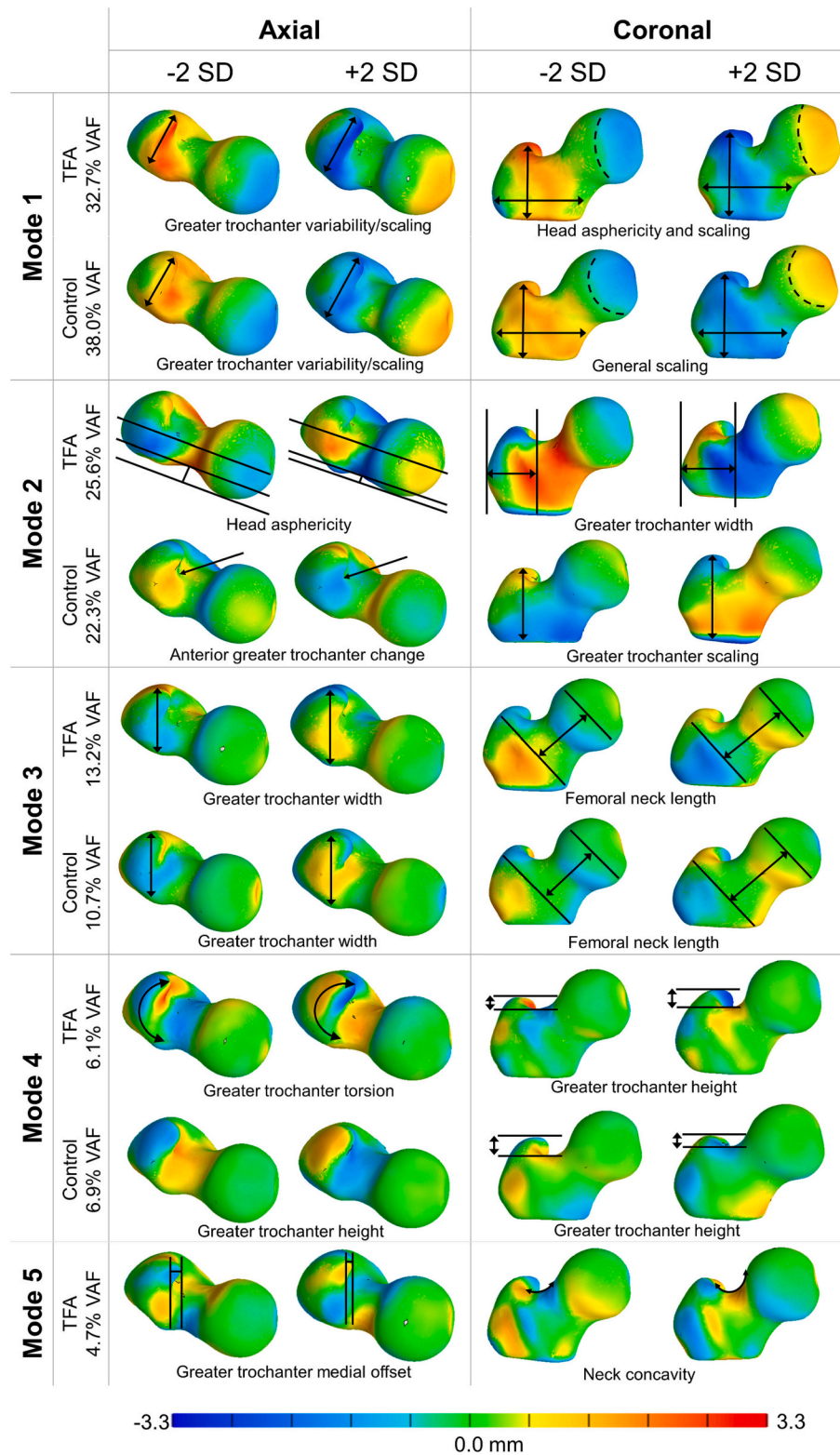
Fig. 5. Significant shape modes for the TFA and control group. The color map femur displays distance from the shape mode to the mean shape for both control and TFA. Mode five shape variation is not included for the control group as it was spurious. Areas of darker red or blue indicate areas which have varied more from the means shape. (For interpretation of the references to color in this figure legend, the reader is referred to the web version of this article.)

remains a primary focus within rehabilitation after limb amputation [64]. However, these results may suggest that abductor strengthening alone may not restore force production as there may be insurmountable mechanical disadvantages due to altered proximal femur morphology.

The current results highlighted unique complex morphological differences in patients with TFA, which were not distinguishable from 2D radiographic measurements alone. This was evidenced by lack of significant differences between groups across 2D radiographic measures despite several 3D shape differences between mean shapes. However, because 2D measures of proximal femur morphology remain the clinical

Table 1

Radiographic measurements made from digitally reconstructed radiographs. Mean ± 1 S.D. 2D radiographic measures of the proximal femur.

View	Measurement	TFA	Control	p-value
Anteroposterior	Femoral neck length	50.3 ± 5.0 mm	48.8 ± 5.6 mm	0.26
	Greater trochanter width	22.9 ± 3.3 mm	21.9 ± 2.9 mm	0.22
	Neck shaft angle	129.2 ± 5.2°	132.7 ± 4.0°	<0.01
	Greater trochanter height	7.8 ± 1.9 mm	6.7 ± 2.1 mm	0.04
Axial	Greater trochanter width	27.1 ± 4.5 mm	27.0 ± 3.9 mm	0.94
	Greater trochanter offset	4.1 ± 1.7 mm	3.8 ± 1.5 mm	0.52
	Greater trochanter (GT) angle	58.3 ± 3.6°	58.4 ± 2.6°	0.96
	Lesser trochanter (LT) angle	21.7 ± 6.8°	21.1 ± 4.6°	0.67
	GT-LT angle	36.6 ± 6.8°	37.3 ± 4.5°	0.64
Frog-leg	Head neck offset	6.8 ± 1.4 mm	7.1 ± 1.9 mm	0.57
	α-angle	55.0 ± 11.0°	54.5 ± 7.3°	0.86

standard and interpretation of 3D SSM results is relatively subjective, correlation of 3D shape modes to 2D radiographic measures is necessary to allow for more objective interpretation of 3D shape results in a clinically translatable manner.

This study possessed several limitations. First, due to the retrospective nature of the design, OA or race were not screened for, which may impact the proximal femur shape distribution [35,65–69]. Second, there are inevitable processing errors due to image segmentation and geometry alignment. However, segmentations were smoothed to remove artifact and aligned via an automated algorithm to reduce root mean square error (relative RMSE <0.0001). Therefore, we interpret any errors associated with processing to be negligible. Third, time since amputation was markedly variable within the TFA group. The inclusion of patients with more short-term prosthesis use would result in the inclusion of femurs with overall less cumulative altered loading compared to those with long-term prosthesis use. However, we expect that this would only serve to minimize the effect of transfemoral prosthesis use on proximal femur shape. Because we found differences in morphology between groups, we do not expect that time since amputation played a significant role on our results. Lastly, due to the novelty of this patient population, the sample size is relatively small; though the sample size is comparable to previous studies which have utilized SSM [28,29]. Future work will aim to expand the image library for patients with TFA.

In summary, we found that the mean proximal femur shape and shape variation were different in patients with TFA compared to able-bodied controls. These differences indicate that altered loading on the

Table 2

Correlations between statistical shape model and digitally reconstructed radiographs. Pearson's correlation coefficients between mode and 2D radiographic measurement for control and TFA group including femoral neck (FN) length, head neck (HN) offset, and novel greater trochanter (GT) and lesser trochanter (LT) measurements, with 95 % confidence intervals given below. Correlations given have $p < 0.05$ and are bolded, where superscript symbols indicate correlation ([+]fairly correlated ($0.25 \leq |r| < 0.50$), [#]moderately correlated ($0.5 \leq |r| < 0.75$), [*]highly correlated ($0.75 \leq |r| \leq 1.0$)). Mode five correlations were not included for the control group as it was spurious.

		Mode 1: GT variability/scaling General scaling		Mode 2: Head asphericity GT scaling/width		Mode 3: Neck length GT width		Mode 4: GT torsion GT height		Mode 5: GT offset Neck concavity
View	2D Measure	Control	TFA	Control	TFA	Control	TFA	Control	TFA	TFA
AP	FN Length	−0.18 (−0.52, 0.20)	−0.20 (−0.52, 0.17)	0.09 (−0.29, 0.44)	0.16 (−0.20, 0.49)	**0.49**[+] (0.15, 0.72)	**0.40**[+] (0.06, 0.66)	−0.01 (−0.38, 0.36)	−0.29 (−0.58, 0.08)	−0.33 (−0.61, 0.03)
	GT Width	0.20 (−0.18, 053)	0.03 (−0.33, 0.38)	−0.03 (−0.39, 0.34)	**0.53**[#] (0.21, 0.74)	**0.63**[#] (0.35, 0.81)	0.24 (−0.13, 0.55)	0.10 (−0.28, 0.45)	**0.37**[+] (0.01, 0.64)	−0.35 (−0.63, 0.01)
	NS Angle	0.07 (−0.30, 0.43)	0.11 (−0.25, 0.45)	0.31 (−0.06, 0.61)	0.17 (−0.20, 0.49)	−0.04 (−0.40, 0.33)	−0.14 (−0.47, 0.22)	−0.11 (−0.46, 0.27)	0.15 (−0.22, 0.48)	**−0.46**[+] (−0.70, −0.13)
	GT Height	0.17 (−0.20, 0.51)	0.26 (−0.11, 0.56)	**−0.42**[+] (−0.68, −0.06)	0.10 (−0.26, 0.44)	−0.08 (−0.43, 0.29)	0.02 (−0.34, 0.37)	**−0.62**[#] (−0.81, −0.33)	**0.45**[+] (0.11, 0.69)	0.11 (−0.26, 0.45)
Axial	GT Width	0.25 (−0.13, 0.56)	0.21 (−0.16, 0.52)	−0.04 (−0.40, 0.33)	**0.48**[+] (0.16, 0.72)	**0.66**[#] (0.39, 0.83)	0.22 (−0.15, 0.53)	0.18 (−0.20, 0.51)	**0.43**[+] (0.09, 0.68)	**−0.43**[+] (−0.68, −0.09)
	GT Offset	0.33 (−0.05, 0.62)	0.32 (−0.03, 0.61)	0.04 (−0.33, 0.40)	0.24 (−0.12, 0.55)	**0.48**[+] (0.14, 0.72)	0.02 (−0.33, 0.38)	0.02 (−0.35, 0.38)	0.27 (−0.10, 0.57)	**−0.58**[#] (−0.77, −0.28)
	GT Angle	−0.24 (−0.56, 0.14)	−0.11 (−0.45, 0.25)	0.07 (−0.31, 0.42)	−0.15 (−0.48, 0.22)	**−0.42**[+] (−0.68, −0.06)	0.00 (−0.36, 0.35)	−0.18 (−0.51, 0.20)	**−0.78**[*] (−0.89, −0.58)	0.11 (−0.25, 0.45)
	LT Angle	0.28 (−0.10, 0.59)	0.16 (−0.20, 0.49)	−0.10 (−0.45, 0.27)	−0.33 (−0.61, 0.03)	0.07 (−0.30, 0.43)	0.31 (−0.05, 0.60)	0.29 (−0.09, 0.59)	−0.21 (−0.53, 0.16)	**0.58**[#] (0.29, −0.28)
	GT-LT Angle	**−0.43**[+] (−0.69, −0.07)	−0.22 (−0.54, 0.14)	0.15 (−0.23, 0.49)	0.25 (−0.11, 0.56)	−0.32 (−0.61, 0.06)	−0.32 (−0.60, 0.04)	**−0.40**[+] (−0.67, −0.04)	−0.20 (−0.51, 0.17)	**−0.53**[#] (−0.74, −0.21)
Frog-leg	HN Offset	−0.24 (−0.56, 0.13)	−0.17 (−0.49, 0.20)	0.34 (−0.03, 0.63)	**−0.54**[#] (−0.75, −0.23)	0.23 (−0.15, 0.55)	0.00 (−0.35, 0.36)	−0.19 (−0.52, 0.19)	−0.16 (−0.49, 0.20)	0.14 (−0.23, 0.47)
	α-angle	0.32 (−0.05, 0.62)	−0.08 (−0.42, 0.28)	−0.35 (−0.64, 0.02)	**0.63**[#] (0.36, 0.80)	−0.10 (−0.45, 0.28)	0.04 (−0.32, 0.38)	0.04 (−0.33, 0.40)	−0.24 (−0.55, 0.13)	**−0.38**[+] (−0.65, −0.03)

amputated limb causes bony morphologic variability of the hip joint, which is corroborated by previous studies demonstrating bony morphological changes due to altered loading [70–72]. These bony morphological changes, including asphericity of the femoral head, can contribute to the development and progression of OA. Thus, our findings indicate that this population would benefit from prostheses alternatives which improve load transmission between the prosthesis and residual limb (e.g., osseointegrated prostheses) [73].

5. Conclusion

To our knowledge, this is the first study to demonstrate that long-term prosthesis use in patients with TFA changes the bony morphology of the hip joint. Better understanding of the effect of long-term prosthesis use on the mechanical and morphological environment of the hip may reveal factors contributing to OA development, thus improving future prosthetic design and targeted interventions. Future work will involve investigation of bilateral differences in proximal femur bony morphology and bilateral muscular differences (e.g., moment arms, volume, composition).

Supplementary data to this article can be found online at https://doi.org/10.1016/j.bone.2023.116752.

CRediT authorship contribution statement

Galen F. Roda: Methodology, software, visualization, formal analysis, writing – original draft, review, and editing. **Jason W. Stoneback:** Data acquisition, writing – review and editing. **David Gimarc:** Data curation, DRR measurement, writing – review and editing. **Brecca M. M. Gaffney:** Conceptualization, investigation, methodology, resources, data curation, writing – review and editing, supervision, project administration.

Declaration of competing interest

There are no competing interests to disclose.

Data availability

Data will be made available on request.

Acknowledgements

References

[1] K. Ziegler-Graham, E.J. MacKenzie, P.L. Ephraim, T.G. Travison, R. Brookmeyer, Estimating the Prevalence of Limb Loss in the United States: 2005 to 2050, Arch. Phys. Med. Rehabil. 89 (2008) 422–429, https://doi.org/10.1016/j.apmr.2007.11.005.

[2] T.R. Vogel, G.F. Petroski, R.L. Kruse, Impact of amputation level and comorbidities on functional status of nursing home residents after lower extremity amputation, J. Vasc. Surg. 59 (2014) 1323–1330.e1, https://doi.org/10.1016/J.JVS.2013.11.076.

[3] E.J. MacKenzie, M.J. Bosse, R.C. Castillo, D.G. Smith, L.X. Webb, J.F. Kellam, A. R. Burgess, M.F. Swiontkowski, R.W. Sanders, A.L. Jones, M.P. McAndrew, B. M. Patterson, T.G. Travison, M.L. McCarthy, Functional outcomes following trauma-related lower-extremity amputation, JBJS 86 (2004) 6, aspx, https://journals.lww.com/jbjsjournal/Fulltext/2004/08000/Functional_Outcomes_Following_Trauma_Related.

[4] R. Gailey, K. Allen, J. Castles, J. Kucharik, M. Roeder, Review of secondary physical conditions associated with lower-limb amputation and long-term prosthesis use, J. Rehabil. Res. Dev. 45 (2008) 15–30, https://doi.org/10.1682/JRRD.2006.11.0147.

[5] P.A. Struyf, C.M. van Heugten, M.W. Hitters, R.J. Smeets, The prevalence of osteoarthritis of the intact hip and knee among traumatic leg amputees, Arch. Phys. Med. Rehabil. 90 (2009) 440–446, https://doi.org/10.1016/j.apmr.2008.08.220.

[6] D.C. Morgenroth, A.C. Gellhorn, P. Suri, Osteoarthritis in the disabled population: a mechanical perspective, PM R. 4 (2012) S20–S27, https://doi.org/10.1016/j.pmrj.2012.01.003.

[7] J. Kulkarni, J. Adams, E. Thomas, A. Silman, Association between amputation, arthritis and osteopenia in british male war veterans with major lower limb amputations, Clin. Rehabil. 12 (1998) 274–279, https://doi.org/10.1191/026921598668452322.

[8] A. Nakamura, S.A. Ali, M. Kapoor, Antisense oligonucleotide-based therapies for the treatment of osteoarthritis: opportunities and roadblocks, Bone 138 (2020), 115461, https://doi.org/10.1016/j.bone.2020.115461.

[9] J.N. Katz, K.R. Arant, R.F. Loeser, Diagnosis and treatment of hip and knee osteoarthritis: a review, JAMA, J. Am. Med. Assoc. 325 (2021) 568–578, https://doi.org/10.1001/jama.2020.22171.

[10] D.T. Felson, Osteoarthritis as a disease of mechanics, Osteoarthr. Cartil. 21 (2013) 10–15, https://doi.org/10.1016/j.joca.2012.09.012.

[11] L. Nolan, A. Lees, The functional demands on the intact limb during walking for active trans-femoral and trans-tibial amputees, Prosthetics Orthot. Int. 24 (2000) 117–125, https://doi.org/10.1080/03093640008726534.

[12] A. Rutkowska-Kucharska, M. Kowal, S. Winiarski, Relationship between asymmetry of gait and muscle torque in patients after unilateral transfemoral amputation, Appl. Bionics Biomech. 2018 (2018), https://doi.org/10.1155/2018/5190816.

[13] M.J. Burke, V. Roman, V. Wright, Bone and joint changes in lower limb amputees, Ann. Rheum. Dis. 37 (1978) 252, https://doi.org/10.1136/ARD.37.3.252.

[14] M. Schaarschmidt, S.W. Lipfert, C. Meier-Gratz, H.C. Scholle, A. Seyfarth, Functional gait asymmetry of unilateral transfemoral amputees, Hum. Mov. Sci. 31 (2012) 907–917, https://doi.org/10.1016/j.humov.2011.09.004.

[15] L. Nolan, A. Wit, K. Dudziński, A. Lees, M. Lake, M. Wychowański, Adjustments in gait symmetry with walking speed in trans-femoral and trans-tibial amputees, Gait Posture. 17 (2003) 142–151, https://doi.org/10.1016/S0966-6362(02)00066-8.

[16] M.P. de Castro, D. Soares, E. Mendes, L. Machado, Plantar pressures and ground reaction forces during walking of individuals with unilateral transfemoral amputation, PM R. 6 (2014) 698–707, https://doi.org/10.1016/j.pmrj.2014.01.019, e1.

[17] S.J. Mellon, K.E. Tanner, Bone and its adaptation to mechanical loading: a review, Http://Dx.Doi.Org/10.1179/1743280412Y.0000000008. 57 (2013) 235–255, https://doi.org/10.1179/1743280412Y.0000000008.

[18] P.C. Noble, G.G. Box, E. Kamaric, M.J. Fink, J.W. Alexander, H.S. Tullos, The effect of aging on the shape of the proximal femur, Clin. Orthop. Relat. Res. (1995) 31–44. http://europepmc.org/abstract/MED/7634721.

[19] J.N. Stabley, R.D. Prisby, B.J. Behnke, M.D. Delp, Chronic skeletal unloading of the rat femur: mechanisms and functional consequences of vascular remodeling, Bone 57 (2013) 355–360, https://doi.org/10.1016/j.bone.2013.09.003.

[20] E. Passmore, H.K. Graham, M.G. Pandy, M. Sangeux, Hip- and patellofemoral-joint loading during gait are increased in children with idiopathic torsional deformities, Gait Posture. 63 (2018) 228–235, https://doi.org/10.1016/J.GAITPOST.2018.05.003.

[21] V.D. Sherk, M.G. Bemben, D.A. Bemben, BMD and bone geometry in transtibial and transfemoral amputees, J. Bone Miner. Res. 23 (2008) 1449–1457, https://doi.org/10.1359/JBMR.080402.

[22] J.C. Baker-LePain, N.E. Lane, Role of bone architecture and anatomy in osteoarthritis, Bone 51 (2012) 197–203, https://doi.org/10.1016/j.bone.2012.01.008.

[23] T.A. Correa, K.M. Crossley, H.J. Kim, M.G. Pandy, Contributions of individual muscles to hip joint contact force in normal walking, J. Biomech. 43 (2010) 1618–1622, https://doi.org/10.1016/J.JBIOMECH.2010.02.008.

[24] M.E. Kersh, S. Martelli, R. Zebaze, E. Seeman, M.G. Pandy, Mechanical loading of the femoral neck in human locomotion, J. Bone Miner. Res. 33 (2018) 1999–2006, https://doi.org/10.1002/jbmr.3529.

[25] D.K. Ryser, R.P. Erickson, T. Cahalan, Isometric and isokinetic hip abductor strength in persons with above-knee amputations, Arch. Phys. Med. Rehabil. 69 (1988) 840–845.

[26] M.C.C. Betancourt, J. Van Meurs, S.B. Zeinstra, F. Rivadeneira, A. Hofman, H. Weinans, A. Uitterlinden, E. Waarsing, Contribution of statistical shape model and predefined geometry parameters in prediction of hip osteoarthritis, Bone 48 (2011) S264, https://doi.org/10.1016/j.bone.2011.03.649.

[27] M.D. Harris, M.C. Shepherd, K. Song, B.M.M. Gaffney, T.J. Hillen, M. Harris-Hayes, J.C. Clohisy, The biomechanical disadvantage of dysplastic hips, J. Orthop. Res. 40 (2022) 1387–1396, https://doi.org/10.1002/jor.25165.

[28] M.D. Harris, M. Datar, R.T. Whitaker, E.R. Jurrus, C.L. Peters, A.E. Anderson, Statistical shape modeling of cam femoroacetabular impingement, J. Orthop. Res. 31 (2013) 1620–1626, https://doi.org/10.1002/jor.22389.

[29] B.M.M. Gaffney, T.J. Hillen, J.J. Nepple, J.C. Clohisy, M.D. Harris, Statistical shape modeling of femur shape variability in female patients with hip dysplasia, J. Orthop. Res. 37 (2019) 665–673, https://doi.org/10.1002/jor.24214.

[30] E.F. Chan, C.L. Farnsworth, J.A. Koziol, H.S. Hosalkar, R.L. Sah, Statistical shape modeling of proximal femoral shape deformities in legg-Calvé-perthes disease and slipped capital femoral epiphysis, Osteoarthr. Cartil. 21 (2013) 443–449, https://doi.org/10.1016/j.joca.2012.12.007.

[31] O. Reikerås, A. Høiseth, in: Femoral Neck Angles in Osteoarthritis of the Hip 53, 2009, pp. 781–784, https://doi.org/10.3109/17453678208992292.

[32] K. Sinusas, Osteoarthritis: diagnosis and treatment, Am. Fam. Physician 85 (2012) 49–56, https://doi.org/10.1136/bmj.1.5222.355-a.

[33] T. Neogi, M.A. Bowes, J. Niu, K.M. De Souza, G.R. Vincent, Y. Goggins, Y. Zhang, D. T. Felson, Magnetic resonance imaging-based three-dimensional bone shape of the

knee predicts onset of knee osteoarthritis: data from the osteoarthritis initiative, Arthritis Rheum. 65 (2013) 2048–2058, https://doi.org/10.1002/ART.37987.

[34] J. Cates, P.T. Fletcher, M. Styner, M. Shenton, R. Whitaker, Shape modeling and analysis with entropy-based particle systems (Including Subser. Lect. Notes Artif. Intell. Lect. Notes Bioinformatics), Lect. Notes Comput. Sci. 4584 (2007) 333–345, https://doi.org/10.1007/978-3-540-73273-0_28. LNCS.

[35] M.M.A. van Buuren, N.K. Arden, S.M.A. Bierma-Zeinstra, W.M. Bramer, N. C. Casartelli, D.T. Felson, G. Jones, N.E. Lane, C. Lindner, N.A. Maffiuletti, J.B. J. van Meurs, A.E. Nelson, M.C. Nevitt, P.L. Valenzuela, J.A.N. Verhaar, H. Weinans, R. Agricola, Statistical shape modeling of the hip and the association with hip osteoarthritis: a systematic review, Osteoarthr. Cartil. 29 (2021) 607–618, https://doi.org/10.1016/j.joca.2020.12.003.

[36] M. Siebelt, R. Agricola, H. Weinans, Y.J. Kim, The role of imaging in early hip OA, Osteoarthr. Cartil. 22 (2014) 1470–1480, https://doi.org/10.1016/J.JOCA.2014.04.030.

[37] A.L. Lenz, N. Krähenbühl, A.C. Peterson, R.J. Lisonbee, B. Hintermann, C. L. Saltzman, A. Barg, A.E. Anderson, Statistical shape modeling of the talocrural joint using a hybrid multi-articulation joint approach, Sci. Rep. 11 (2021), https://doi.org/10.1038/s41598-021-86567-7.

[38] M.D. Harris, A.L. Kapron, C.L. Peters, A.E. Anderson, Correlations between the alpha angle and femoral head asphericity: implications and recommendations for the diagnosis of cam femoroacetabular impingement, Eur. J. Radiol. 83 (2014) 788–796, https://doi.org/10.1016/j.ejrad.2014.02.005.

[39] P.R. Atkins, Y. Shin, P. Agrawal, S.Y. Elhabian, R.T. Whitaker, J.A. Weiss, S. K. Aoki, C.L. Peters, A.E. Anderson, Which two-dimensional radiographic measurements of cam femoroacetabular impingement best describe the three-dimensional shape of the proximal Femur? Clin. Orthop. Relat. Res. 477 (2019) 242–253, https://doi.org/10.1097/CORR.0000000000000462.

[40] C. Metz, Digitally Reconstructed Radiographs, Utr. Univ. Master's T, 2005.

[41] J.C. Clohisy, J.C. Carlisle, R. Trousdale, Y.J. Kim, P.E. Beaule, P. Morgan, K. Steger-May, P.L. Schoenecker, M. Millis, Radiographic evaluation of the hip has limited reliability, Clin. Orthop. Relat. Res. 467 (2009) 666–675, https://doi.org/10.1007/s11999-008-0626-4.

[42] J. Cates, S. Elhabian, R. Whitaker, ShapeWorks: Particle-based Shape Correspondence and Visualization Software, 1st ed., Elsevier Ltd, 2017 https://doi.org/10.1016/B978-0-12-810493-4.00012-2.

[43] C. Goodall, Procrustes methods in the statistical analysis of shape, J. R. Stat. Soc. Ser. B 53 (1991) 285–321, https://doi.org/10.1111/j.2517-6161.1991.tb01825.x.

[44] T. Cootes, C. Taylor, D. Cooper, J. Graham, Active shape models - their training and application, Comput. Vis. Image Underst. 61 (1995) 38–59.

[45] S.B. Franklin, D.J. Gibson, P.A. Robertson, J.T. Pohlmann, J.S. Fralish, Parallel analysis: a method for determining significant principal components, J. Veg. Sci. 6 (1995) 99–106, https://doi.org/10.2307/3236261.

[46] H. Abdi, L.J. Williams, Principal component analysis, Wiley interdiscip. RevComput. Stat. 2 (2010) 433–459, https://doi.org/10.1002/wics.101.

[47] J. Cates, P.T. Fletcher, M. Styner, M. Shenton, R. Whitaker, Foundations of Clinical Research: Applications to Practice, 4th ed., F.A. Davis Company, 2020.

[48] D. Curran-Everett, Explorations in statistics: confidence intervals, Am. J. Physiol. - Adv. Physiol. Educ. 33 (2009) 87–90, https://doi.org/10.1152/ADVAN.00006.2009/SUPPL_FILE/ADVANCES_STATISTICS_CODE_CIS.R.

[49] S.M.H.J. Jaegers, J.H. Arendzen, H.J. de Jongh, Prosthetic gait of unilateral transfemoral amputees: a kinematic study, Arch. Phys. Med. Rehabil. 76 (1995) 736–743, https://doi.org/10.1016/S0003-9993(95)80528-1.

[50] K.K. Patterson, W.H. Gage, D. Brooks, S.E. Black, W.E. McIlroy, Evaluation of gait symmetry after stroke: a comparison of current methods and recommendations for standardization, Gait Posture. 31 (2010) 241–246, https://doi.org/10.1016/j.gaitpost.2009.10.014.

[51] B. Burkett, J. Smeathers, T. Barker, Walking and running inter-limb asymmetry for paralympic trans-femoral amputees, a biomechanical analysis, Prosthetics Orthot. Int. 27 (2003) 36–47, https://doi.org/10.3109/03093640309167975.

[52] R. Ganz, J. Parvizi, M. Beck, M. Leunig, H. Nötzli, K.A. Siebenrock, Femoroacetabular impingement: a cause for osteoarthritis of the hip, Clin. Orthop. Relat. Res. 417 (2003) 112–120, https://doi.org/10.1097/01.BLO.0000096804.78689.C2.

[53] M. Kowalczuk, M. Yeung, N. Simunovic, O.R. Ayeni, Does femoroacetabular impingement contribute to the development of hip osteoarthritis? A systematic review, Sports Med. Arthrosc. 23 (2015) 174–179, https://doi.org/10.1097/JSA.0000000000000091.

[54] J.F. Ramírez, J.A. Isaza, I. Mariaka, J.A. Vélez, Analysis of bone demineralization due to the use of exoprosthesis by comparing Young's modulus of the femur in unilateral transfemoral amputees, Prosthetics Orthot. Int. 35 (2011) 459–466,

[55] V.J. Harandi, D.C. Ackland, R. Haddara, L.E.Cofré Lizama, M. Graf, M.P. Galea, P. V.S. Lee, in: Individual Muscle Contributions to Hip Joint-Contact Forces During Walking in Unilateral Transfemoral Amputees With Osseointegrated Prostheses, 2020, pp. 1071–1081, https://doi.org/10.1080/10255842.2020.1786686.

[56] F.A. Gottschalk, M. Stills, The Biomechanics of Trans-femoral Amputation, 1994.

[57] T.M. Köhler, S. Blumentritt, F. Braatz, M. Bellmann, The impact of transfemoral socket adduction on pelvic and trunk stabilization during level walking – a biomechanical study, Gait Posture. 89 (2021) 169–177, https://doi.org/10.1016/J.GAITPOST.2021.06.024.

[58] D.W.W. Heitzmann, J. Leboucher, J. Block, M. Günther, C. Putz, M. Götze, S. I. Wolf, M. Alimusaj, The influence of hip muscle strength on gait in individuals with a unilateral transfemoral amputation, PLoS One 15 (2020), e0238093, https://doi.org/10.1371/JOURNAL.PONE.0238093.

[59] S.M.H.J. Jaegers, J.H. Arendzen, H.J. de Jongh, Prosthetic gait of unilateral transfemoral amputees: a kinematic study, Arch. Phys. Med. Rehabil. 76 (1995) 736–743, https://doi.org/10.1016/S0003-9993(95)80528-1.

[60] E. Tazawa, Analysis of torso movement of trans-femoral amputees during level walking, Prosthetics Orthot. Int. 21 (1997) 129–140, https://doi.org/10.3109/03093649709164541.

[61] A. Amaro, F. Amado, J.A. Duarte, H.J. Appell, Gluteus medius muscle atrophy is related to contralateral and ipsilateral hip joint osteoarthritis, Int. J. Sports Med. 28 (2007) 1035–1039, https://doi.org/10.1055/s-2007-965078.

[62] G. Valente, F. Taddei, I. Jonkers, Influence of weak hip abductor muscles on joint contact forces during normal walking: probabilistic modeling analysis, J. Biomech. 46 (2013) 2186–2193, https://doi.org/10.1016/J.JBIOMECH.2013.06.030.

[63] K. Song, B.M.M. Gaffney, K.B. Shelburne, C. Pascual-Garrido, J.C. Clohisy, M. D. Harris, Dysplastic hip anatomy alters muscle moment arm lengths, lines of action, and contributions to joint reaction forces during gait, J. Biomech. 110 (2020), 109968, https://doi.org/10.1016/J.JBIOMECH.2020.109968.

[64] R. Isac Vieira, S. Cristina Tonon da Luz, K. Priscila Bender dos Santos, E. Gonçalvez Junior, P. Vanessa Coelho Campos, Physiotherapy intervention during pre and post-prosthetic fitting of lower limb amputees: a systematic review, (n.d.). doi: 10.5935/0104-7795.20170019.

[65] V. Pedoia, M.A. Samaan, G. Inamdar, M.C. Gallo, R.B. Souza, S. Majumdar, Study of the interactions between proximal femur 3d bone shape, cartilage health, and biomechanics in patients with hip osteoarthritis, J. Orthop. Res. 36 (2018) 330–341, https://doi.org/10.1002/JOR.23649.

[66] J.H. Waarsing, R.M. Rozendaal, J.A.N. Verhaar, S.M.A. Bierma-Zeinstra, H. Weinans, A statistical model of shape and density of the proximal femur in relation to radiological and clinical OA of the hip, Osteoarthr. Cartil. 18 (2010) 787–794, https://doi.org/10.1016/J.JOCA.2010.02.003.

[67] G. Inamdar, V. Pedoia, J. Rossi-Devries, M.A. Samaan, T.M. Link, R.B. Souza, S. Majumdar, MR study of longitudinal variations in proximal femur 3D morphological shape and associations with cartilage health in hip osteoarthritis, J. Orthop. Res. 37 (2019) 161–170, https://doi.org/10.1002/JOR.24147.

[68] G.W. Gill, Racial variation in the proximal and distal femur: heritability and forensic utility, J. Forensic Sci. 46 (2001) 15049J, https://doi.org/10.1520/JFS15049J.

[69] A.E. Nelson, F. Liu, J.A. Lynch, J.B. Renner, T.A. Schwartz, N.E. Lane, J.M. Jordan, Association of Incident Symptomatic hip Osteoarthritis with Differences in hip shape by active shape modeling: the Johnston County osteoarthritis project, Arthritis Care Res. (Hoboken) 66 (2014) 74–81, https://doi.org/10.1002/ACR.22094.

[70] S. Mayes, A.R. Ferris, P. Smith, A. Garnham, J. Cook, Bony morphology of the hip in professional ballet dancers compared to athletes, Eur. Radiol. 27 (2017) 3042–3049, https://doi.org/10.1007/S00330-016-4667-X/FIGURES/5.

[71] R. Agricola, J.H.J.M. Bessems, A.Z. Ginai, M.P. Heijboer, R.A. Van Der Heijden, J. A.N. Verhaar, H. Weinans, J.H. Waarsing, The development of cam-type deformity in adolescent and young male soccer players, Am. J. Sports Med. 40 (2012) 1099–1106, https://doi.org/10.1177/0363546512438381.

[72] U. Pettersson, P. Nordström, H. Alfredson, K. Henriksson-Larsén, R. Lorentzon, Effect of high impact activity on bone mass and size in adolescent females: a comparative study between two different types of sports, Calcif. Tissue Int. 2000 673 (67) (2014) 207–214, https://doi.org/10.1007/S002230001131.

[73] B.M.M. Gaffney, N.W. Vandenberg, H.C. Davis-Wilson, C.L. Christiansen, G. F. Roda, G. Schneider, T. Johnson, J.W. Stoneback, Biomechanical compensations during a stand-to-sit maneuver using transfemoral osseointegrated prostheses: a case series, Clin. Biomech. 98 (2022), 105715, https://doi.org/10.1016/J.CLINBIOMECH.2022.105715.